DUST AND ICE OCCURRENCE RATIOS OVER DUST SOURCES OBSERVED BY SPACE/GROUND BASED ACTIVE REMOTE SENSOR

Yoshitaka Jin[1], Kenji Kai[1], Hajime Okamoto[2], Yuichiro Hagihara[2], Hongfei Zhou[3]

[1]*Graduate school of Environmental Studies, Nagoya University, Furo-cho, Nagoya 461-8601, JAPAN, E-mail:jin.yoshitaka@a.mbox.nagoya-u.ac.jp*
[2]*Research Institute for Applied Mechanics, Kyushu University, 6-1 Kasugakouen, Kasuga, 816-8580, JAPAN*
[3]*Xinjiang Institute of Ecology and Geography, CAS, Urumqi, 830011, CHINA*

ABSTRACT

Dust Occurrence Ratio (DOR) and Ice Occurrence Ratio (IOR) over the Saharan and Taklimakan Deserts are investigated in this study. Aerosols such as dust act as ice nuclei and affect on the Earth's radiation budget as indirect effect. The spatial distributions of such aerosols and formed clouds are not well known. In order to overcome the problems, we used Cloud-Aerosol Lidar and Infrared Pathfinder Satellite Observation (CALIPSO), CloudSat, and ECMWF reanalysis data for extracting the aerosol and cloud profiles. The ground-based lidar observation was also carried out in north Taklimakan Desert to validate the satellite analysis. The purpose of this study is to clarify the change of the IOR according to the DOR. The result shows that the DOR over the Asian Deserts was higher and broader than that over the Saharan Desert. It means there were the Asian dust more frequently compared to the Saharan dust at the low temperatures. The IOR of the Taklimakan region were higher than those of the Saharan region for all temperatures and the DOR were also higher. We also examined the relationship between the DOR and IOR using those for the Saharan and Taklimakan Deserts. The result shows that the increasing rate of the IOR with respect to the DOR was increased at lower temperature. The result of the ground-based lidar analysis was consistent with the result of the satellite analysis.

1. INTRODUCTION

Atmospheric dust is an important source of ice cloud formation. In general, pure water freeze via homogeneous ice nucleation in the low temperature ($T < -40$). However, the freezing can only occur by heterogeneous ice nulceation in the temperature range of mixed phase clouds ($-40 < T < 0$). The numerous studies of laboratory experiments and observations have shown that the dust acts as ice nuclei (IN) effectively [1; 2; 3; 4]. Aerosols such as the dust modify the number concentration and effective radius of clouds by acting as IN and it makes change of the precipitation rate and optical depth, single scattering albedo, emissivity, and lifetime of clouds, and therby affects on the Earth's radiation budget [5; 6]. However, such aerosol indirect effects have a large uncertainty in the current knowledge [7]. This is attributed to the lack of information where and how high the aerosols acting as IN distribute and the fact that the microphysical processes regarding ice nuclei are not understood yet. Because the aerosol has the various chemical compositions and partice size distributions as well as the large temporal and spatial variations in the atmosphere, it makes the observation of the three dimensional aerosol distributions difficult.

In this study, we focused on the dust acting as IN originating from the Taklimakan Desert because it has been pointed out that the dust serves as IN more effective than the dust from other sources. For example, Wiacek et al., (2009, 2010) performed forward trajectory calculations and showed that the Taklimakan dust can easily be lifted up to the higher altitude than the dust of other sources and therefore potentially the biggest impact of mineral dust is predicted to be on mixed phase clouds[8; 9] . Choi et al., (2010) investigated the supercooled cloud fraction in the cloud using Cloud-Aerosol Lidar with Orthogonal Polarization (CALIOP) on board Cloud-Aerosol Lidar and Infrared Pathfinder Satellite Observation (CALIPSO) and suggested that the supercooled cloud fraction over the Asian Desert was the lowest around the globe due to the effective glaciation by the dust [10]. However, the ground-based observation on site related to IN has rarely been conducted so far. The goal of this study is to clarify the change of ice occurrence ratio (IOR) according to dust occurrence ratio (DOR). We used 1-year satellite (CALIPSO/CloudSat) and reanalysis (ECMWF) data as well as the ground-based lidar data in the field. The result showed that the increasing rate of the IOR with respect to the DOR was increased at lower temperature.

2. OBSERVATION AND DATA ANALYSIS

2.1. Ground-based lidar observation

We carried out a lidar observation in north of the Taklimakan Desert in March $23-25$, 2009 [11; 12]. The lidar employed a Nd:YAG laser (pulse energy: 300 mJ, pulse repetition rate: 10 Hz, first and second harmonic) for the light source. The 355 mm Schmidt-Cassegrain telescope was used for focusing backscattered light from scatters. The received light was dispersed into 532 and $1,064$ nm by the beam splitter and the former was divided into cross and parallel components respect to polarization plane of the incient light by polarization prism. The photomultiplier tubes and avalanche photodiode were used for return signal detection at 532 and $1,064$ nm, respectively. Therefore, the lidar can measure the vertical profile from the ground surface to a height of 120 km every five minutes with a vertical resolution of 7.5 m and produce 532

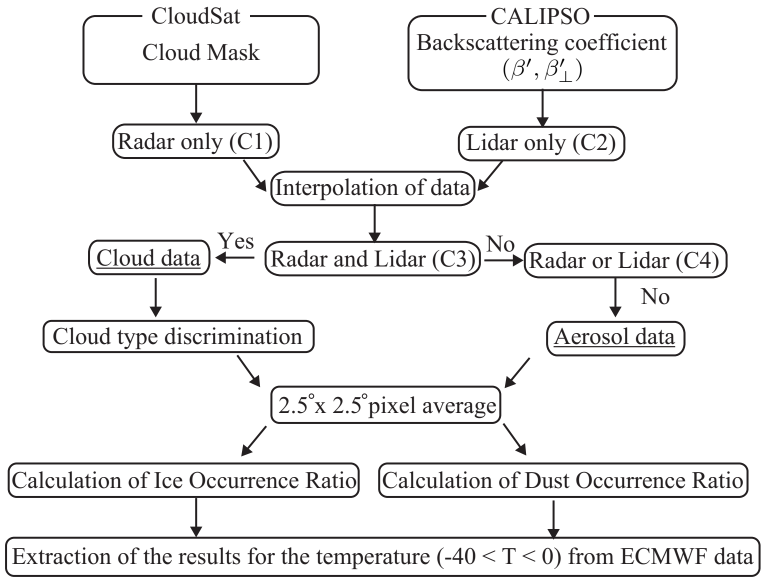

Figure 1: Flow chart of the satellite analysis in this study.

and $1,064$ nm backscatters and a depolarization ratio at 532 nm as same as CALIOP.

2.2. Method of satellite data analysis

Figure 1 shows the satellite data analysis flow chart of this study. To investigate the IOR and DOR, we must determine the profile that contains cloud. We used CALIPSO and CloudSat data for the determination. Hagihara et al., (2010) developed the folloing four cloud mask schemes: (1) CloudSat only (C1), (2) CALIPSO only (C2), (3) CloudSat and CALIPSO (C3) in which both C1 and C2 detect cloud, and (4) CloudSat or CALIPSO (C4) in which at least C1 or C2 detect cloud [13]. These schemes are based on the cloud masks used in the shipborne 95GHz cloud radar and lidar observation in the western Pacific Ocean near Japan [14]. We used the profile of C3 scheme to analyze for only cloud data and the residual profile other than C4 scheme for aerosol data.

The scheme C1 utilizes the CPR level 2B GEOPROF cloud mask. It considers signal-to-noise ratio (SNR), spatial continuity, and horizontal averaging and contains confidence level values ranging between 0 and 40 [15]. We used the bin data if the confidence level more than 20 and it's false detection estimated via CALIPSO comparison is 5%. The results are vertically averaged and therefore each profile has the same altitude registration with respect to the geoid data. The vertical resolution is 240 m with 83 bins, and horizontal resolution is 1.1 km as same as the original CloudSat resolution. We identified the bin as cloud where the cloud fraction was more than 50%. The scheme C2 utilizes the CALIOP Lidar Level 1B (version 2.01) total backscattering coefficient at 532 nm (β'). As the first criterion, the scheme considers a threshold value which is determined by the background noise, molecular signal, and altitude. The spatial continuity test was applied using the surrounding bins in the secondly criterion to calculate the cloud fraction. We identified the bin as cloud where the cloud fraction was more than 50% likewise C1. The C1 and C2 results were interpolated onto the common grid. The CALIPSO data were averaged within the CloudSat footprint and therefore had same vertical and horizontal resolutions as C1 grid. We used as the cloud data if a bin was identified as cloud in both C1 and C2 schemes and the aerosol data if a profile was not identified as cloud at least C1 or C2 schemes in the same grid.

After the detection of the cloud, the cloud type discrimination was carried out for the cloud data using the algorithm developed by [16]. Based on the relationship between the ratio of the total attenuated backscattering coefficients for two vertically consective cloud bins and the volume depolarization ratio (VDP), following cloud particle types could be discriminated: (1) warm water, (2) super cooled water, (3) randomly oriented ice crystals (3D ice), and (4) horizontally oriented plates (2D plate). We calculated the ice occurrence frequency by counting the bin number of 3D ice, 2D plate, and mixture of them. Consequently, IOR was defined as the ratio of the ice occurrence frequency to all cloud bin number. The IOR and aerosol data were averaged in 2.5 x 2.5 degree pixel. The attenuated backscattering coefficient for cross ($\beta'_{\perp}$) and parallel ($\beta'_{||}$) components were used for aerosol data. The averaged data was still contaminated by the random noise. We calculated a SNR for each bin and if the SNR less than 3, the bin was eliminated from the data. We calculated VDR and if it's value was more than 0.1, we identified the bin as a dust and calculated the dust occurrence frequency. In a similar manner of IOR, DOR was defined as the ratio of dust occurrence frequency to all aerosol bin number in the 2 °C interval. Finally, calculated IOR and DOR were extracted for the ranging ($-40 < T < 0$) using the temperature from the ECMWF data. The calculation period was from June 2006 to May 2007.

3. RESULTS AND DISCUSSION

Figure 2 shows a DOR and Cloud Occurrence Frequency (COF) for the temperature between -20 and -10 °C for the calculation period. The COF is the number of bins that were classified into the cloud data. In Figure 2 (a), there were the high DOR around the Saharan and Asian Deserts. The DOR over the Asian Desert was higher and broader than that over the Saharan Desert. It means there were the Asian dust more frequently compared to the Saharan dust at the low temperatures. Asian dust is led to a higher potential due to their higher elevation, which makes their surface potential temperature much hotter, and higher latitude, which is preconditioned to reach higher neutral buoyancy levels by large ascent mechanisms [9]. In Figure 2 (b), there were high COF over the Asian dust sources and Siberian regions. The higher COFs were also seen over the west Saharan dust sources compared to the other African regions except for around Ethiopia.

The IOR were calculated for the two regions that were depicted by white rectangles in Figure 2 (b). The rectangle regions are the west Saharan dust sources (15 $-$ 35°N, 10°W$-$10°E) and the Taklimakan dust sources (35 $-$ 45°N, 75 $-$ 90°E). The results of averaged IOR and DOR as a function of temperature are shown in Figure 3. For comparison with non dust contaminated region, we also calculated the IOR for near Antarctic (45 $-$ 55°S, 20 $-$ 40°W). As you can see in Figure 3, the IOR (DOR) of all regions were increasing (decreasing) as the temperature decreased. The Taklimakan dust source region had higher IORs than near Antarctic region for all temperatures, while the Saharan region did only more than -20 °C. The IORs of the Taklimakan region were higher than those of the Saharan region for all temperatures and the DORs were also higher as mentioned earlier. The DORs of the Saharan region were less than 3% below about -20 °C, while below about -30 °C for the Taklimakan region. We examined the relationship between DOR and IOR using those for the dust source regions. The averaged DOR and IOR for each 8 °C are plotted and connected the regions with straight lines in Figure 4. The IOR and DOR for the Taklimakan region had the higher value than those for the Saharan region as shown in Figure 3. The IOR were increasing as the DOR were increased for all temperatures and it suggests that atmospheric dust can act as ice nuclei. It should be noted that the gradient of connected line was increasing as the temperature decreased. It means that dusts were act as ice nuclei more effectively at lower temperatures. This results is corresponding to the findings of previous study [17] that ice nulei concentration is increasing as the temperature decreases. In laboratory studies, the deposition freezing is generally not observed for more than -20 °C [18]. If the dusts have not experienced chemical coatings,

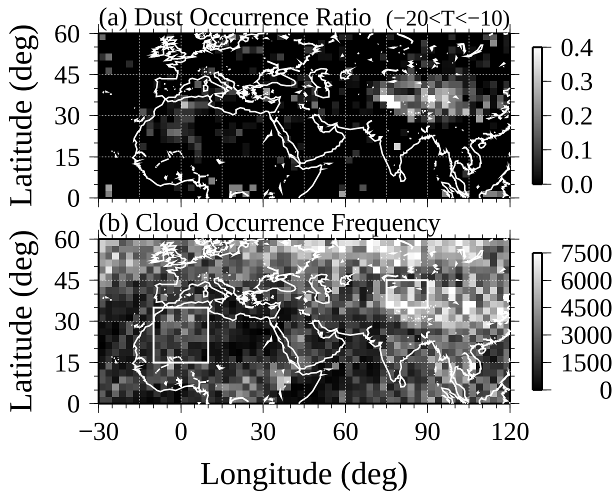

Figure 2: Spatial distributions of (a) Dust Occurrence Ratio and (b) Cloud Occurrence Frequency for the temperature range ($-20 < T < -10$).

immersion and contact freezings can occur at the temperature. Because the calculated relative humidities respect to water for the bin classified as the cloud were almost below 100% (not shown in this paper), it was thought that the contact freezing possibly occurred. For colder than -20 °C, it is considered that the deposition freezing occurred as well as contact freezing because the deposition freezing was more efficient for this temperature.

Figure 5 shows the occurrence frequency of the cloud VDR and the DOR as a function of the temperature observed by the ground-based lidar. As you can see, the VDR of almost clouds were more than 0.1 even above -40 °C although there were few clouds for above -20 °C. It means that the most of observed clouds were comprised of ice crystal. Meanwhile, the DOR was more than 0.05 for above -60 °C and rapidly increasing from -30 °C. Although the time series depolarization ratio is not shown in this paper (but presented Figure 4(b) in [12]), the depolarization ratio of the aerosols near the clouds were almost over 0.1 where temperatures were above -30 °C (below about 7 km AMSL). This result is consistent with the results of satellite analysis. However, it is needed to analyze more ground-based lidar data to validate the satellite data.

ACKNOWLEDGMENTS

The authors are grateful to CALIPSO and CloudSat science team providing the data used in this study.

REFERENCES

1. Isono, K., et al. 1959: *J. Meteor. Soc. Japan*, **37**, pp. 211-233.
2. DeMott, P. J., et al. 2003: *Geophys. Res. Lett.*, **30**, 1732, doi:10.1029/2003GL017410.
3. Sassen, K., et al. 2003: *Geophys. Res. Lett.*, **30**, 1633, doi:10.1029/2003GL017371.

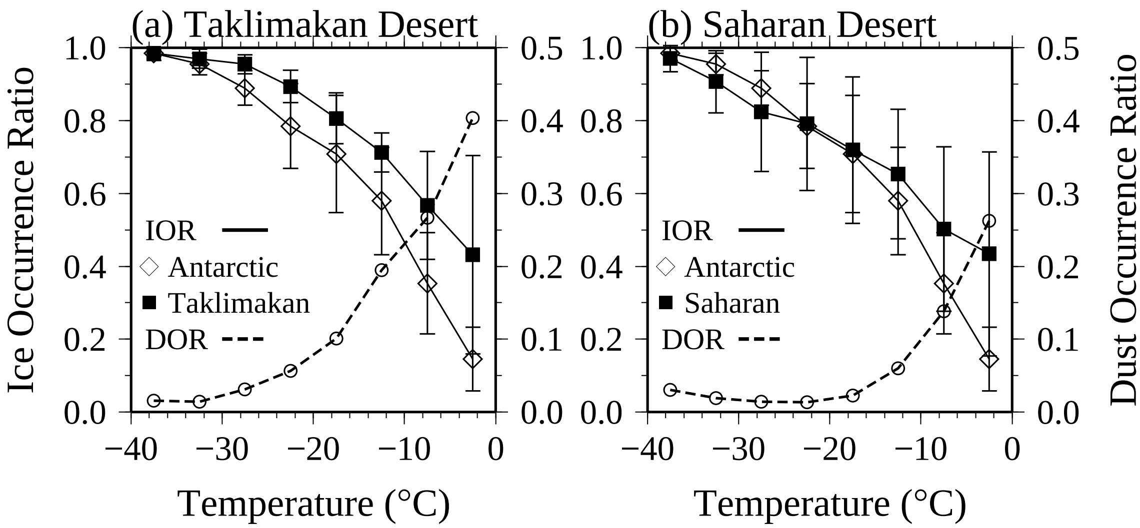

Figure 3: Ice Occurrence Ratio (IOR) and Dust Occurrence Ratio (DOR) as a function of the temperature over (a) the Taklimakan Desert and (b) the Saharan Desert. IOR near the Antarctic is also depicted for comparison.

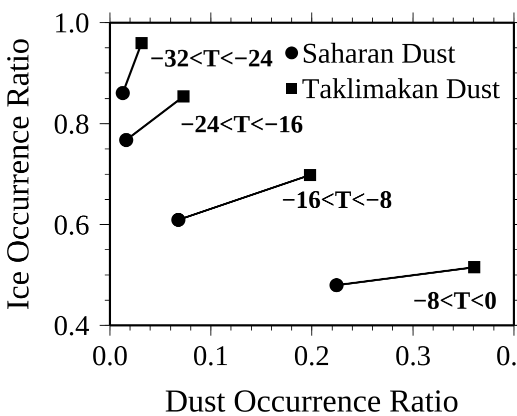

Figure 4: Relationship between Dust Occurrence Ratio and Ice Occurrence Ratio for the four temperature ranges.

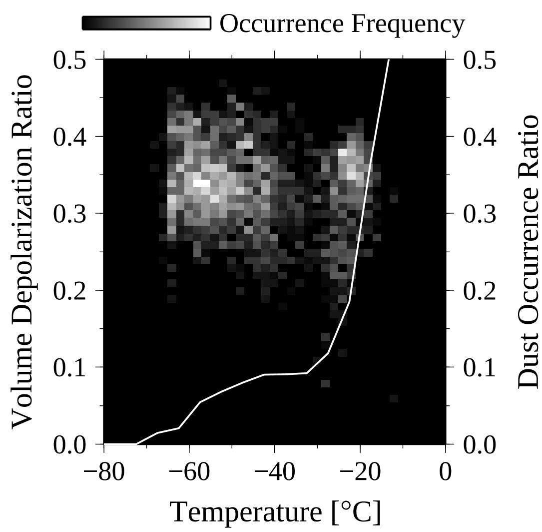

Figure 5: Occurrence frequency of the volume depolarization ratio of clouds and dust occurrence ratio as a function of the temperature obaserved by ground-based lidar.

4. Sakai, T., et al. 2003: *Appl. Opt.*, **42**, pp. 7130-7116.
5. Twomey, S. A., et al. 1984: *Tellus*, **36B**, pp. 356-366.
6. Ebert, E. E. and Curry, J. A. 1992: *J. Geophys. Res.*, **97**, pp. 3831-3836.
7. Forster, et al. Cambridge University Press, Cambridge, 2007.
8. Wiacek, A., and Peter, T. 2009: *Geophys. Res. Lett.*, **36**, L17801, doi:10.1029/2009GL039429.
9. Wiacek, A., et al. 2010: *Atmos. Chem. Phys.*, **10**, pp. 8649-8667.
10. Choi, Y.-S., et al. 2010: *Proc. Natl. Acad. Sci.*, **107**, pp. 11211-6.
11. Jin, Y., et al. 2010: *SOLA*, **6**, pp. 121-124.
12. Jin, Y., et al. 2010: *Proc. of SPIE*, **7856**, pp. 785609-1-785609-10.
13. Hagihara, Y., et al. 2010: *J. Geophys. Res.*, **115**, D00H33.
14. Okamoto, H., et al. 2007: *J. Geophys. Res.*, **112**, D08216.
15. Marchand, R., et al. 2008: *J. Atmos. Ocean Tech.*, **25**, pp. 519-533.
16. Yoshida, R., et al. 2010: *J. Geophys. Res.*, **115**, D00H32.
17. Fletcher, N. H. Cambridge University Press, New York, 1962.
18. Field, P. R., et al. 2006: *Atmos. Chem. Phys.*, **6**, pp. 2991-3006.